Journal of ELECTRONIC MATERIALS, Vol. 49, No. 9, 2020
https://doi.org/10.1007/s11664-020-08176-w

TOPICAL COLLECTION: 18TH CONFERENCE ON DEFECTS (DRIP XVIII)

A Cathodoluminescence Study on the Diffusion Length in AlGaInP/InGaP/AlInP Solar Cell Heterostructures

SHABNAM DADGOSTAR,[1,3] CANTIA BELLOSO CASUSO,[1] OSCAR MARTÍNEZ,[1] MANUEL HINOJOSA,[2] IVÁN GARCÍA,[2] and JUAN JIMÉNEZ[1]

1.—GdS-Optronlab Group, Dept. Física de la Materia Condensada, Universidad de Valladolid, Paseo de Belén, 19, 47011 Valladolid, Spain. 2.—Instituto de Energía Solar, ETSI de Telecomunicacíon, Universidad Politécnica de Madrid, 28040 Madrid, Spain. 3.—e-mail: shabnam.dadgostar@uva.es

The diffusion length of minority carriers in a *p*-doped InGaP layer is derived from the cathodoluminescence (CL) intensity profiles. Two procedures are used. First, the CL profile is recorded along a line crossing the intersection between a thin metallic mask and the semiconductor; a second approach consists of the measurement of the intensity profile around an intentional scratch on the surface of the sample. A longer diffusion length is measured when using the metallic mask as compared with the scratch. We discuss the role of non-radiative recombination centers in the reduction of the diffusion length around the scratch. The temperature dependence of the diffusion length is also measured, and the length is found to decrease with temperature.

Key words: Minority carriers, diffusion length, optoelectronic devices, cathodoluminescence, III–V multi-junctions, III–V solar cell

INTRODUCTION

The ternary alloy $In_xGa_{1-x}P$ is an interesting material that can be grown lattice-matched to GaAs for a composition of $In_{0.49}Ga_{0.51}P$. It is used in various devices, such as light-emitting diodes, laser diodes, photodetectors, and multi-junction solar cells. The efficiency of multi-junction solar cells based on this material exceeds 40% and is predicted to reach 50% in the near future.[1–3]

Minority carrier transport properties are crucial for the operation of optoelectronic devices; therefore, the minority carrier diffusion length (L_{Diff}) is a necessary parameter for the design and optimization of these devices. The diffusion length depends on the band structure of the material, the crystal quality, alloy composition, doping concentration, and the presence of defects, either impurities or intrinsic. Cross-sectional electron beam-induced current (EBIC) and transport imaging in a scanning electron microscope are two techniques applied to measure the minority carrier diffusion length. However, the electric fields and surface recombination are challenges with the EBIC method,[4,5] while a 2D CCD camera is necessary for the transport imaging technique.[6,7] Cathodoluminescence (CL) has also been used to measure the minority carrier diffusion length in semiconductors.[8] Two experimental approaches are used to determine diffusion length.[9] In the first approach, a metallic mask is deposited on the semiconductor surface. This mask must be thin enough to permit the penetration of the electron beam across the metal to reach the semiconductor, where the electron–hole pairs are generated and recombined. The metal layer, however, must be thick enough to block the CL emission emerging. The diffusion length is measured by scanning the e-beam along a line perpendicular to the metal/semiconductor border. When the e-beam is separated from the metal/semiconductor border, a distance equal to or shorter than the diffusion

(Received November 28, 2019; accepted April 29, 2020; published online May 12, 2020)

length, some carriers can reach the border, recombining in the unmasked semiconductor region, and the emitted CL can be collected.[10] The second approach uses a defect, such as an isolated dislocation or other extended defect, to evaluate the diffusion length. Extended defects usually behave as non-radiative recombination centers. Around the defects, the CL intensity declines dramatically due to the diffusion of carriers toward the defect, where they recombine in a non-radiative manner, giving a dark CL contrast. Therefore, the diffusion length might be estimated from the CL intensity profile collected around the defect.[11,12]

In this work, we estimate the lateral minority carrier diffusion length in a *p*-type $In_{0.49}Ga_{0.51}P$ layer using the two approaches, a gold mask and a scratch line. The impact of the presence of defects is analyzed.

EXPERIMENTAL

The samples used for measurements were lattice-matched double AlGaInP/InGaP heterostructures deposited on a GaAs substrate 2° miscut toward the (111) B plane. Growth was carried out in a horizontal low-pressure metalorganic vapor-phase epitaxy (MOVPE) reactor (AIX 200/4). The precursors for the group-III elements are TMGa and TMIn, AsH_3 and PH_3 are used for the group-V, and $DTBSi_2$, DETe and DMZn are the dopant precursors. The layer of interest is a 1000-nm-thick $In_{0.49}Ga_{0.51}P$:Zn sandwiched between a 250-nm-thick $Al_{0.104}Ga_{0.416}In_{0.48}P$:Zn layer and a 190-nm-thick $In_{0.49}Ga_{0.51}P$:Si layer. The nominal doping concentrations for the *p*-type and *n*-type layers are 1×10^{17} cm^{-3} and 1×10^{18} cm^{-3}, respectively. A schematic of the structure is shown in Fig. 1a.

The CL measurements were carried out in a LEO 1530 (Carl Zeiss) field-emission scanning electron microscope (FESEM) equipped with a MonoCL2 (Gatan, Oxford, UK) CL system. The detection was performed with a Peltier-cooled CCD detector. Figure 1b shows a SEM image of the surface of the sample, where one can see the gold/semiconductor border. The measurement was performed by scanning the beam transversely to the borderline (along the red line in Fig. 1b) and recording the CL spectrum at each position, achieving a hyper-spectral line scan. The gold layer was 50 nm thick, which permits excitation of the CL for beam energies above 10 keV. A typical CL spectrum is shown in Fig. 1c. The sharp peak at 660 nm (1.877 eV at 80 K) corresponds to the conduction (CB)-to-valence band (VB) emission in the InGaP layer, while the low-intensity peak at 620 nm (2 eV) arises from the CB-to-VB transition in the AlGaInP top layer. The transmittance of the 50-nm-thick gold layer in this spectral range is below 3%.[13] The thickness of the gold layer is a critical point of these measurements. One must look for a compromise between the thickness of the gold layer and the e-beam energy (generation volume and penetration depth). This problem is not present when one scans the e-beam across the scratch or any other extended defect, although in this case the size of the generation volume with respect to the defect should be taken into account. Figure 1d shows the SEM image of the sample with a line scratch on its surface. The electron beam was scanned across the scratch line (along the red line), and the CL spectrum was recorded at each position. The e-beam energy was optimized to achieve the best conditions for the measurement of the diffusion length in each case. The temperature was varied from 80 K to 300 K.

RESULTS AND DISCUSSION

Monte Carlo calculations for different e-beam energies were carried out to estimate the penetration depth across the Au/AlGaInP/InGaP sample structure and the lateral extension of the generation volume. Figure 2a, b, and c presents the energy loss distributions for 7 keV, 13 keV and 20 keV e-beams. At 7 keV, the e-beam is stopped by the Au layer, and a very weak CL signal is collected. By increasing the beam energy (E_b) to 13 keV, the volume generation is mainly constrained to the AlGaInP layer, while at 20 keV the volume generation extends toward the InGaP layer simultaneously with a higher lateral extension. The spectra collected for different e-beam energies on top of the gold layer, at a distance of ≈ 1 μm from the gold border, are shown in Fig. 2d. For E_b up to 15 keV, the generation volume is mainly located in the AlGaInP top layer; the carriers generated in this layer can diffuse laterally and recombine in the AlGaInP layer. They can also drift as a result of the built-in potential from the top layer into the InGaP layer, where they diffuse laterally and recombine giving the 660 nm CL peak. One should consider two ways to reach the mask border in the InGaP layer.[8] In the first path, by lateral diffusion across the AlGaInP top layer, surface recombination plays a major role, as revealed by the very weak luminescence intensity emitted by the AlInGaP top layer; the spectra of Fig. 2d do not show the AlGaInP layer emission at 620 nm. The CL emission from diffused carriers along the AlGaInP layer is not observed because the surface recombination prevents sufficient minority carrier diffusion to give an appreciable CL signal (620 nm). For low E_b, the carriers are generated in the top AlGaInP layer (Fig. 2a). The population of carriers reaching the InGaP layer is low; therefore, the lateral flux of minority carriers that reaches the metal border is too low to produce significant CL intensity, and so the diffusion length is underestimated. As more electrons arrive in the InGaP layer, by increasing E_b, the lateral electron flux should increase, enhancing the CL signal generated by the diffused electrons emerging from the metal mask.

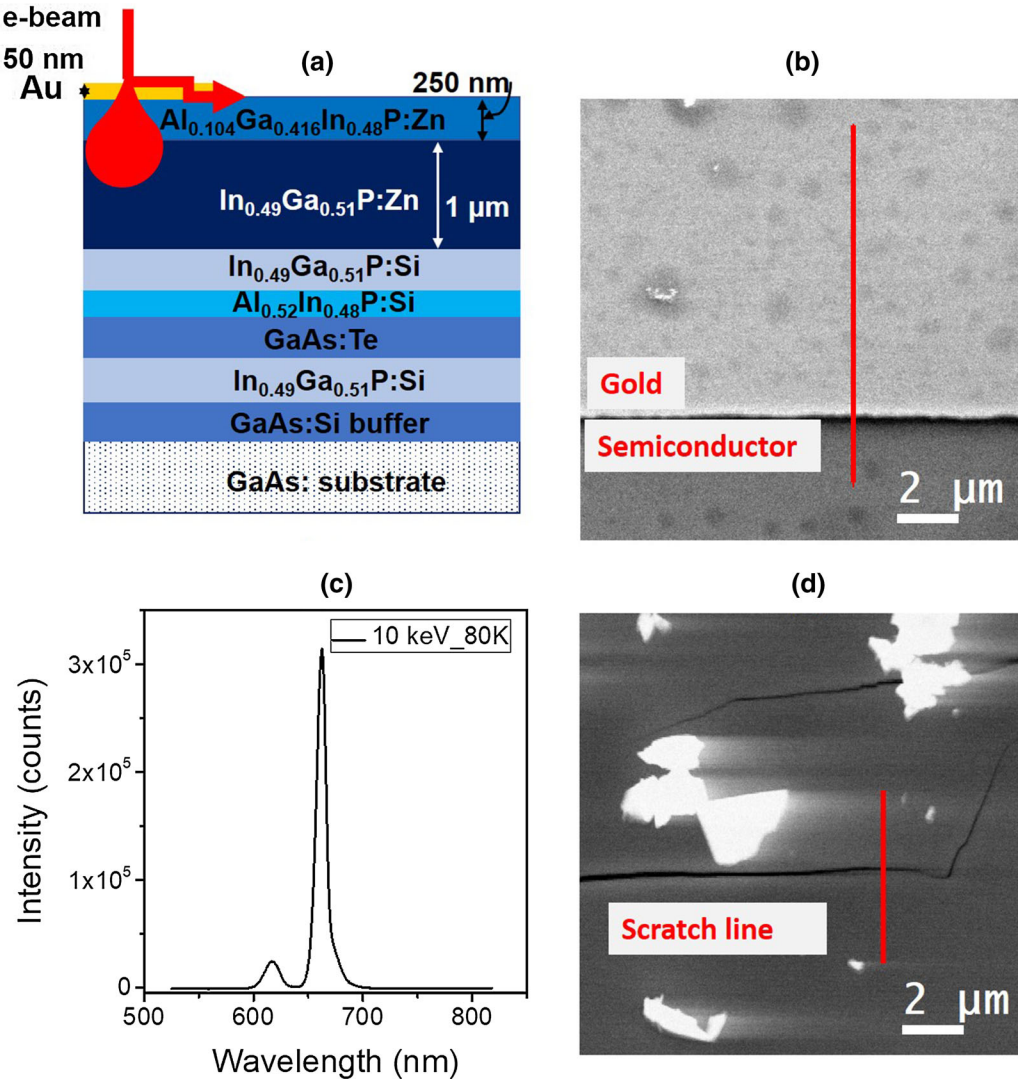

Fig. 1. (a) Schematic of the multi-junction (cross-section). (b) To measure the diffusion length, the electron beam scanned a line normal to the gold/semiconductor border. The red line indicates the scan direction. (c) Typical recorded CL spectrum at 80 K for 10 keV e-beam energy. (d) SEM image of a scratch line with the scanning line (Color figure online).

The CL intensity profiles for different e-beams are plotted in log scale in Fig. 3a. One observes that the slope of these plots depends on the e-beam energy. To calculate the diffusion length, the lateral extension of the generation volume must be considered. The primary electron range is the parameter limiting the spatial resolution; therefore, it must be considered when fitting the experimental data for obtaining the diffusion length from the CL intensity profile along a line scan crossing the metal/semiconductor border. To consider the impact of the generation volume, the lateral radius (taken at 90% energy loss) was considered. The generation volumes for different $E_b$values were calculated using open-access Casino software.[14] Taking account of the electron range in the equation describing the CL intensity as a function of the distance of the e-beam to the metal mask edge (Fig. 3a):

$$I_{CL} = I_0 \exp\left(\frac{-(x + r_v)}{L_{Diff}}\right), \quad (1)$$

where L_{Diff} represents the diffusion length, r_v is the excitation volume radius, and x is the distance of the e-beam from the mask edge. The spectrum shape is preserved all along the scanning line, which permits us to assume that there are no inhomogeneities associated with the presence of defects.

The diffusion length (L_{Diff}) was estimated for different e-beam energies (E_b). The result is shown in Fig. 3b, where one observes the dependence of L_{Diff} with E_b, the measured diffusion length increases with E_b. The measured diffusion length at 300 K increases from 0.3 μm under 7 keV excitation to 1.4 μm for 20 keV excitation. This dependence is related to the generation volume and certainly to the carrier generation rates, in fact, the CL intensity measured shall be related to the

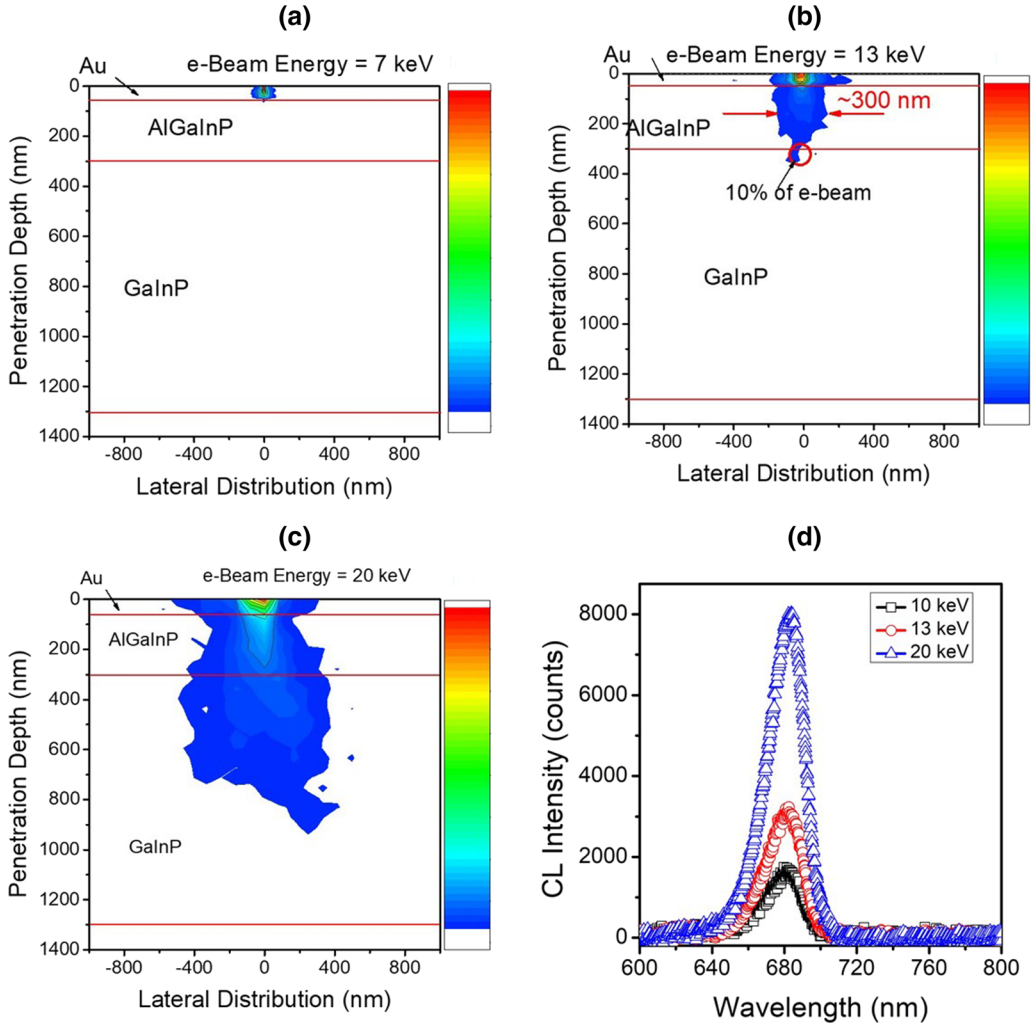

Fig. 2. The Monte Carlo modeling of the absorbed energy cross-section for (a) 7 keV, (b) 13 keV and (c) 20 keV e-beam energy (the scale bar ranges from 0% to 100% energy loss). The bar indicates the absorbed energy from 5% (red) to 90% (dark blue). (d) CL spectra (300 K) for 10 keV, 13 keV and 20 keV on top of the gold layer 1 μm from the gold border (Color figure online).

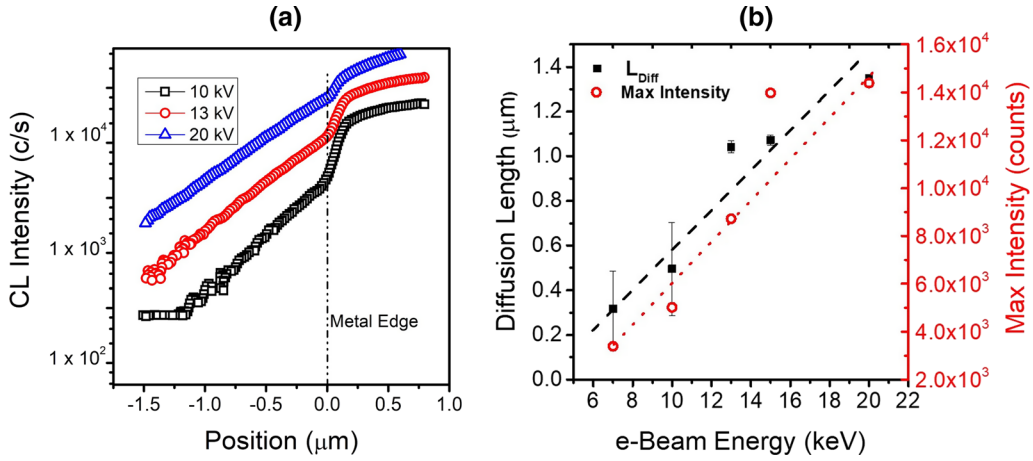

Fig. 3. (a) CL intensity profiles across the gold/semiconductor border at 300 K and different e-beam energies. (b) Diffusion lengths (black squares) and the maximum recorded CL (red circles) as a function of the e-beam energy (300 K) (Color figure online).

flux of carriers reaching the metal border, which will be higher for higher carrier generation rates. One can establish a relation between L_{Diff} and the maximum CL intensity (I_{CL}), which depends on E_{b}. In fact, one observes that the measured L_{Diff} increases with I_{CL} (Fig. 3b).

Figure 4 illustrates the variation in the diffusion length and CL intensity as a function of temperature between 80 K and 300 K for 13 keV e-beam energy. The results indicate a reduction in diffusion length with an increase in temperature from 1.37 μm at 80 K to about 1.0 μm at room temperature. One can observe the L_{Diff} profiles of both the 660 nm (1.877 eV) band, corresponding to the InGaP layer (Fig. 4), and the 620 nm (2 eV) band, corresponding to the AlGaInP top layer (Fig. 4, inset). The diffusion in the top layer is almost suppressed by the surface recombination, while the surface recombination does not disturb the diffusion in the InGaP layer. Considering the relation between L_{Diff} and T:

$$L_{\mathrm{Diff}} = \sqrt{\frac{k_{\mathrm{B}}T}{e}\mu\tau}, \tag{2}$$

where μ is the mobility, τ is the carrier lifetime, k_{B} is the Boltzmann constant, and T is the temperature, the decrease of L_{Diff} with T is due to a reduction of the $\mu\tau$ factor that overbalances the increase in T. One can expect a reduction in the lifetime, assuming the contribution of non-radiative recombination centers; on the other hand, a reduction in mobility due to acoustic phonon scattering with increasing temperature in an alloy of these characteristics could account for such a decrease in diffusion length.[12] The values obtained are in line with those reported in recent works.[7]

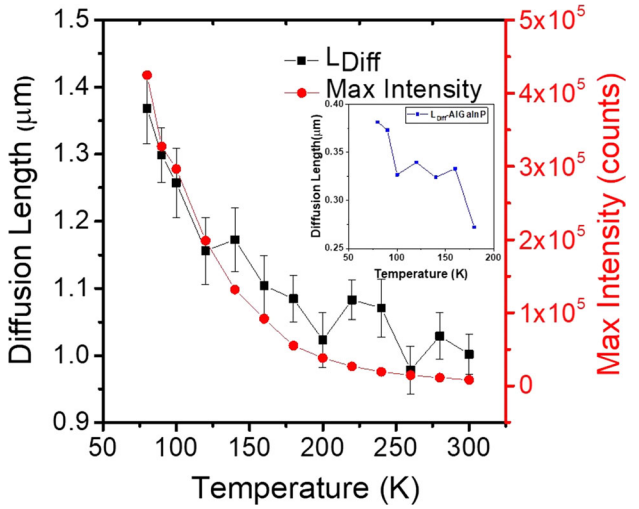

Fig. 4. Diffusion length (black squares) and CL intensity (red circles) as a function of temperature in the interval of 80–300 K for an e-beam energy of 13 keV. The inset shows the temperature-dependent diffusion length of minority carriers in the AlGaInP top layer. Lines are visual guides (Color figure online).

Alternatively, we studied the diffusion length by recording the CL spectra around a scratch. The scratch gives a dark contrast in the CL image because of the non-radiative recombination. The carrier lifetime in the neighborhood of the scratch is limited by the diffusion rate of the electrons toward the defect. The scratch line was not fully quenched. In fact, the emissions from the top layer and the InGaP layer were still observed when the e-beam was on the scratch line, which accounts for relatively low non-radiative recombination activity, suggesting a low concentration of deep levels in the scratch. The e-beam was scanned in a transverse direction to the scratch line, and the diffusion length was calculated from the exponential decay of the CL intensity as a function of the distance to the scratch line (Fig. 5).

The estimated diffusion length is shorter than the measured length when using the metallic mask. This reduction can be attributed to the presence of non-radiative recombination centers surrounding the scratch, which were created by the mechanical deformation induced by the scratch. Also, the band bending around the defect could contribute to the drift of minority carriers toward the scratch, where they recombine in a non-radiative manner. The non-radiative recombination centers would be responsible for a reduction in the effective carrier lifetime, which in the absence of surface recombination can be expressed as:

$$\frac{1}{\tau_{\mathrm{eff}}} = \frac{1}{\tau_{nr}} + \frac{1}{\tau_{r}}. \tag{3}$$

Note that the two main recombination mechanisms deduced from the CL spectrum are the CB-VB radiative recombination (660 nm) and non-radiative recombination at deep levels, as no other recombination channels are seen in the CL spectrum. On the other hand, we have seen that the surface recombination does not affect the emission of the InGaP layer. The role of the deep levels generated by the plastic deformation induced by the scratch is also supported by the asymmetrical CL profiles at the two sides of the scratch, which is a consequence of the differences in distribution of the deep levels at each side of the scratch line (Fig. 5a). Note that band bending around the defect can be generated by the presence of deep levels capturing majority carriers; therefore, minority carrier drift can occur under the influence of the electric field, resulting in a shorter effective diffusion length. In the example in Fig. 5, this effect is relatively small; however, for deeper scratches generating more damage, one observes changes in the CL intensity profile around the scratch that may be associated with minority carrier drift by the electric field associated with the scratch.

The temperature-dependent results show a reduction in both CL intensity and diffusion length with

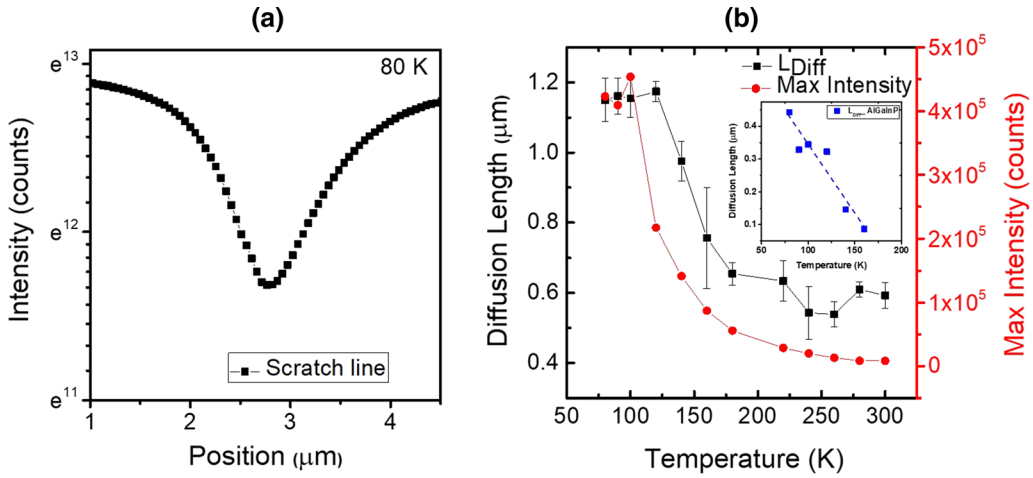

Fig. 5. (a) CL intensity at the vicinity of the scratch line under 13 keV e-beam energy and 80 K. (b) Temperature-dependent diffusion length (black squares) and maximum CL intensity (red circles) around the scratch line. The inset shows the temperature-dependent diffusion length of minority carriers in the AlGaInP top layer. The lines are visual guides (Color figure online).

increasing temperature. Here, the diffusion length decreases from 1.1 μm to 0.6 μm respectively at 80 K and 300 K (Fig. 4b). This behavior suggests that the effective carrier lifetime is reduced with T, which is consistent with the presence of deep levels, for which the recombination rate increases with T. Therefore, one must be cautious in estimating the diffusion length, which can depend on the distribution of defects around the scratch or extended defect, such as a decorated dislocation, or a scratch surrounded by deep levels.

CONCLUSIONS

We have presented a study of the in-plane minority carrier diffusion length in AlGaInP/InGaP heterostructures using spectrally resolved CL. The measurements were carried out on clean material using a metallic mask, and on damaged material using a scratch as the carrier sink. The experimental conditions, e-beam energy and temperature, were studied.

The diffusion length around a scratch was shorter than that measured across the metallic mask in clean material, which was explained in terms of the formation of deep levels that reduce the effective lifetime of the minority carriers and the electric field associated with the scratch.

Finally, the diffusion length was found to decrease with T in both cases, suggesting that carrier lifetime is reduced by capture by deep levels, and scattering by phonons is reducing the mobility.

ACKNOWLEDGMENTS

This work was supported by Project VA283P18 (Junta de Castilla y Leon) and Project ENE2017-89561-C4-3-R (Spanish Ministry of Economics and Competitiveness), and the European Fund for Regional Development (FEDER).

REFERENCES

1. A.W. Bett, S.P. Philipps, S.S. Essig, S. Heckelmann, R. Kellenbenz, V. Klinger, M. Niemeyer, D. Lackner, and F. Dimroth, *28th Eur. Photovolt. Sol. Energy Conf. Exhib.* (2013). https://doi.org/10.4229/28thEUPVSEC2013-1AP.1.1.
2. F. Dimroth, T.N.D. Tibbits, M. Niemeyer, F. Predan, P. Beutel, C. Karcher, E. Oliva, G. Siefer, D. Lackner, P. Fus-Kailuweit, A.W. Bett, R. Krause, C. Drazek, E. Guiot, J. Wasselin, A. Tauzin, and T. Signamarcheix, *IEEE J. Photovolt.* 6, 343 (2016).
3. M. Green, K. Emery, Y. Hishikawa, W. Warte, E. Dunlop, D.H. Levi, and A.W.Y. Ho-Baillie, *IEEE Prog. Photovolt Res. Appl.* 25, 3 (2017).
4. M. Niemeyer, J. Ohlmann, A.W. Walker, P. Kleinschmidt, R. Lang, T. Hannappel, F. Dimroth, and D. Lackner, *J. Appl. Phys.* 122, 115702 (2017).
5. O. Marcelot, S.I. Maximenko, and P. Magnan, *IEEE Trans. Electron Devices* 61, 2437 (2014).
6. D.R. Luber, F.M. Bradley, N.M. Haegel, M.C. Talmadge, M.P. Coleman, and T.D. Boone, *Appl. Phys. Lett.* 88, 163509 (2006).
7. F.J. Schultes, T. Christian, R. Jones-Albertus, E. Pickett, K. Alberi, B. Fluegel, T. Liu, P. Misra, A. Sukiasyan, H. Yuen, and N.M. Haegel, *Appl. Phys. Lett.* 103, 242106 (2013).
8. D. Araújo, G. Oelgart, J.D. Ganière, and F.K. Reinhart, *J. Appl. Phys.* 76, 342 (1994).
9. J. Jimenez and J.W. Tomm, *Spectroscopic Analysis of Optoelectronic Semiconductors* (Switzerland: Springer International Publishing, 2016).
10. H.A. Zarem, P.C. Sercel, J.A. Lebens, L.E. Eng, A. Yariv, and K.J. Vahala, *Appl. Phys. Lett.* 55, 1647 (1989).
11. D. Araújo, G. Oelgart, J.D. Ganière, and F.K. Reinhart, *Appl. Phys. Lett.* 62, 2992 (1993).
12. N. Ino and N. Yamamoto, *Appl. Phys. Lett.* 93, 232103 (2008).
13. A. Axelevitch, B. Gorenstein, and G. Golan, *Phys. Procedia* 32, 1 (2012).
14. D. Drouin, A.R. Couture, D. Joly, X. Tastet, V. Aimez, and R. Gauvin, *Scanning* 29, 92 (2007).